Microsatellite markers and cytoplasmic sequences reveal contrasting pattern of spatial genetic structure in the red algae species complex Mazzaella laminarioides

Marie-Laure Guillemin, Myriam Valero, Kennia Morales Collio, Ramona Pinochet Sanchez, Miguel Henríquez Espinosa, Andrea X. Silva

MICROSATELLITE MARKERS AND CYTOPLASMIC SEQUENCES REVEAL CONTRASTING PATTERN OF SPATIAL GENETIC STRUCTURE IN THE RED ALGAE SPECIES COMPLEX *MAZZAELLA LAMINARIOIDES*

Marie-Laure Guillemin

Instituto de Ciencias Ambientales y Evolutivas, Facultad de Ciencias, Universidad Austral de Chile, Casilla 567, Valdivia, Chile.

CNRS, Sorbonne Universités, UPMC University Paris VI, UMI 3614, Evolutionary Biology and Ecology of Algae, Station Biologique de Roscoff, CS 90074, Place G. Tessier, 296888 Roscoff, France.

Email: marielaure.guillemin@gmail.com

Phone: +56 063 222 1703

Myriam Valero

CNRS, Sorbonne Universités, UPMC University Paris VI, UMI 3614, Evolutionary Biology and Ecology of Algae, Station Biologique de Roscoff, CS 90074, Place G. Tessier, 296888 Roscoff, France.

Kennia Morales Collio

Instituto de Ciencias Ambientales y Evolutivas, Facultad de Ciencias, Universidad Austral de Chile, Casilla 567, Valdivia, Chile.

Ramona Pinochet Sanchez

Instituto de Ciencias Ambientales y Evolutivas, Facultad de Ciencias, Universidad Austral de Chile, Casilla 567, Valdivia, Chile.

Miguel Henríquez Espinosa

Instituto de Ciencias Ambientales y Evolutivas, Facultad de Ciencias, Universidad Austral de Chile, Casilla 567, Valdivia, Chile.

Andrea X. Silva

AUSTRAL-*omics*, Facultad de Ciencias, Universidad Austral de Chile, Casilla 567, Valdivia, Chile.

Running Title: Genetic discordance in *Mazzaella laminarioides*

Abstract: *Mazzaella laminarioides* (Bory) is a common haploid-diploid red alga that forms dense beds. This alga has a wide distribution range, covering 3,500km of the Chilean coast, but is restricted to high rocky intertidal zones. Recently, the existence of three highly divergent genetic lineages was demonstrated for this taxon, and two cytoplasmic markers were used to determine that these lineages are distributed in strict parapatry. Here, using 454 next-generation sequencing, we developed polymorphic microsatellite loci that cross amplify in all three cytoplasmic lineages. Six sites (i.e. two sites within each lineage) were analyzed using nine microsatellite loci. Our work shows that, although substantial cytoplasmic differentiation occurs within *M. laminarioides*, the microsatellite loci did not retrieved three nuclear genetic clusters as expected. Indeed, while the northernmost and southernmost cytoplasmic lineages form two strongly divergent nuclear groups characterized by diagnostic alleles, the third cytoplasmic lineage did not form a third nuclear independent group. It is possible that inter-lineage gene exchange has occurred, particularly at sites along the contact zone between the different cytoplasmic lineages. This nuclear-cytoplasmic incongruence in *M. laminarioides* could be explained by incomplete lineage sorting of the nuclear genes or asymmetric introgressive hybridization between the lineages. Finally, highly significant heterozygote deficiencies (suggesting occurrence of intergametophytic selfing) were observed in the three small northernmost sites while the large southernmost sites generally approached panmixia.

Keywords: Chile, gene flow, intergametophytic selfing, microsatellites, Rhodophyta, species complex

List of abbreviations:

COI, cytochrome c oxidase sub-unit1

cpDNA, chloroplast DNA

ENSO, El Niño Southern Oscillation

HRMA, high resolution melting analysis

LD, linkage disequilibrium

mtDNA, mitochondrial DNA

PCA, principal component analysis

RAPD, random amplified polymorphic DNA

rbcL, large subunit of the ribulose-1,5-bisphosphate carboxylase/oxygenase enzyme

Introduction

The Chilean coast is mostly linear from north to south and characterized by very dynamic and regionalized tectonic, oceanographic and climatic processes (Thiel et al. 2007, Guillemin et al. 2015). These coastal and oceanic features have led to contrasted pattern of marine biodiversity distributed over three main biogeographic regions (Camus 2001, Thiel et al. 2007). The particularities of the Chilean coast have stimulated a strong

73 interest in deciphering the phylogeographic patterns of the marine realm in this region
74 and studies have accumulated rapidly during the last five years (see for review in
75 invertebrates: Haye et al. 2014 and in seaweeds: Guillemin et al. 2015). More specifically,
76 these two reviews report the use of molecular markers in species that cross the
77 biogeographic boundaries to compare concordance among phylogeographic and
78 biogeographic breaks. In seaweeds, based on the occurrence of divergent mitochondrial
79 lineages, several putative cryptic species were uncovered along the Chilean coast: in
80 *Lessonia* (Tellier et al. 2009), *Durvillaea* (Fraser et al. 2009), *Adenocystis* (Fraser et al.
81 2013), *Mazzaella* (Montecinos et al. 2012) and *Nothogenia* (Lindstrom et al. 2015). Most
82 of these studies were only based on the analysis of the cytoplasmic genomic compartment,
83 except for *Lessonia* in which comparison of divergence at nuclear and cytoplasmic
84 markers supported the same pattern (Tellier et al. 2009). Furthermore, in this last case,
85 nuclear microsatellites markers were used to demonstrate that the two cryptic species did
86 not share any alleles and were, thus, reproductively isolated (Tellier et al. 2011).
87 However, conflicting geographic patterns between mitochondrial and nuclear
88 genetic markers have been observed when demographic asymmetries produce dissimilar
89 movement in the two marker types or when different selective pressures affect the
90 mitochondrial and the nuclear genome (Toews and Brelsford 2012). For example, in the
91 barnacle *Notochthamalus scabrosus,* Zakas et al. (2014) reported that the nuclear genome
92 homogeneity throughout the central and northern regions of Chile contrasted with the
93 strong mitochondrial divergence pattern described previously (Zakas et al. 2009). They
94 concluded that there is little reason to treat the two mitochondrial groups as distinct
95 species. In contrast with invertebrates, dispersal is generally limited to less than a few

96 kilometers in seaweed and such pattern of nuclear homogeneity along the Chilean coast is
97 not expected in those organisms (Kinlan and Gaines, 2003). It is thus interesting to test
98 for algae cryptic species, which were defined on the basis of divergent cytoplasmic
99 lineages, if their pattern of nuclear genetic structure is congruent with their cytoplasmic
100 divergence.

101 *Mazzaella laminarioides* is a haploid-diploid rocky shore species that forms dense
102 beds in high intertidal zones. This carrageenophyte is an economically important resource
103 in Chile and is harvested from natural populations by small fishing communities
104 (Buschmann et al. 2001). *M. laminarioides* is non-buoyant and is considered to be a poor
105 disperser (Faugeron et al. 2001). The species distribution range encompasses a high
106 variety of environmental conditions as it covers 3,500km (28-56°S) of Chilean coastline
107 (Thiel et al. 2007). Using two cytoplasmic genes (COI, mitochondrial and *rbc*L,
108 chloroplast), Montecinos et al. (2012) revealed strong genetic structure within *M.*
109 *laminarioides* with the existence of three divergent genetic lineages distributed along the
110 Chilean coast. They reported the presence of a northern lineage from 28°S to 32°S, a
111 central lineage from 34°S to 37°S, and a southern lineage from 39°S to 56°S. Guillemin
112 et al. (2015) confirmed that the three lineages are distributed in strict parapatry with sharp
113 phylogeographic breaks of a few kilometers in width. However, the presence of
114 reproductive barriers has not been tested between these three lineages.

115 In *M. laminarioides*, the three cytoplasmic lineages were separated for the *rbc*L
116 by 0.6 to 1.0% divergence and for COI by 2.6 to 7.8% divergence and no cytoplasmic
117 incongruence was observed (Montecinos et al. 2012). In red algae, where both plastid and
118 mitochondria DNA maternal inheritance have been observed (Zuccarello and West 2011),

119 cytoplasmic incongruence have generally been related to events of interspecific
120 hybridization (Destombe et al. 2010). These results suggest that strong reproductive
121 barriers probably evolved between the three lineages of *M. laminarioides* limiting
122 hybridization even in the contact zones. Indeed, in the Rhodophyta, laboratory crosses
123 between phylogenetic species have generally revealed complete reproductive
124 incompatibility that correlates with cytoplasmic genetic distances (Brodie and Zuccarello
125 2006, Zuccarello and West 2011 and reference therein). In the three species complex
126 thoroughly studied (i.e. *Spyridia*, *Bostrychia,* and *Mastocarpus*), the experiments showed
127 that strains sharing the same chloroplastic haplotypes (rubisco spacer) were always fully
128 compatible while strains differing by only 0.6 to 2.1% were not able to be crossed
129 (Zuccarello and West 2002, Zuccarello and West 2003, Zuccarello et al. 2005).
130 We can predict that, in agreement with plastid and mitochondrial information, the
131 nuclear genome should present strong genetic discontinuities with no or very limited gene
132 flow among the three cytoplasmic lineages of *M. laminarioides*. In this context, we
133 developed nine microsatellite markers for the red alga *M. laminarioides* in order to
134 confirm the existence of nuclear genetic structure and to test for potential hybridization
135 between the three previously described parapatric cytoplasmic lineages.
136
137 Material and Methods
138 *Development of microsatellite markers* - In order to construct the 454 libraries, a single
139 haploid (i.e. a female gametophyte) specimen was used as the source of DNA for each
140 three cytoplasmic lineages of *M. laminarioides*. Samples from Fray Jorge
141 (30°40'S/71°42'W), Constitución (35°19'S/72°26'W) and Chiloe (41°52'S/71°01'W) were

142 used for the northern, central and southern lineage respectively (Montecinos et al. 2012).
143 DNA was extracted following the protocol described by Saunders (1993); slight
144 modifications were made according to Faugeron et al. (2001). PicoGreen^{TM} fluorescence
145 enhancement (Ahn et al. 1996) was used to test DNA quality and quantity. DNA
146 sequencing was performed using a 454 GS Junior Titanium Series (Roche) at the
147 AUSTRAL-omics Core-Facilities. Briefly, each DNA sample was tagged using different
148 multiplex identifiers (MIDs). DNA library fragments were captured onto beads and
149 clonally amplified within individual emulsion droplets. Amplified fragments from all
150 three lineages were evenly mixed and sequenced on 3 PicoTiterPlates. Library
151 preparation, amplification, and sequencing were carried out following the manufacturer
152 protocols (Roche Diagnostics Corporation, Branford, Connecticut USA). The assembly
153 of the reads was performed using the MIRA (Chevreux et al. 1999) and CAP3 (Huang
154 and Madan 1999) software programs. In order to determine which contigs correspond to
155 nuclear sequences, nucleotide BLAST (http://blast.ncbi.nlm.nih.gov/Blast.cgi) searches
156 were performed using the complete mitochondrial genome of *Chondrus crispus* (25.836
157 bp NC_001677) and using the complete plastid genome of *C. crispus* (180.086 bp,
158 HF562234). Moreover, in order to identified loci sequenced in more than one of our three
159 454 libraries, we performed nucleotide BLAST searches between the three cytoplasmic
160 lineages contig files.

161 Nucleotide repeats from di- to hexa-nucleotides were identified using
162 MSATCOMMANDER (Faircloth 2008). Generally, the BLAST searches between the
163 three cytoplasmic lineages contig files show that the same microsatellite locus have been
164 sequenced in more than one of our three 454 libraries (see Table S1). For microsatellite

loci present in more than one of our three 454 libraries, alignment between the different cytoplasmic lineages were performed in GENEIOUS R6 for each locus (Biomatters Ltd.). For 30 loci with a high number of repetitions (at least 7 repetitions) and long flanking regions located in the nuclear contigs, primers pairs were designed using GENEIOUS R6 (Biomatters Ltd.). When the same microsatellite locus was encountered in more than one 454 library (see Table S1) the primer pairs were designed within the more conserved part of the flanking region. All loci for which alignment between the different cytoplasmic lineages were performed showed clear homologies in their flanking regions.

Following primer design, PCR cross amplification of all three lineages was performed; for this, three individuals from Fray Jorge, three individuals from Constitución, and three individuals from Chiloe were used. For the 20 loci that amplified successfully in all three lineages, high resolution melting analysis (HRMA, Mackay et al. 2008) was used to make a preliminary assessment of variability. For each lineage, three sites were tested: Fray Jorge, Puerto Obscuro, and Maitencillo for the northern lineage; Topocalma, Constitución, and Concepción for the central lineage; and Pucatrihue, Chiloe, and Punta Arenas for the southern lineage. Fifteen haploid individuals from each site were used. The COI regions of all of the haploid samples were previously sequenced in the study of Montecinos et al. (2012). The HRMA analyses showed that twelve loci were polymorphic for *M. laminarioides*.

Genotyping – The twelve polymorphic loci were used to genotype 96 diploid individuals sampled from Caleta Sauce (SAU, N=16), Mina Talca (MIT, N=18), Montemar (MTM, N=16), Lebu (LEB, N=16), Pilolcura (PIL, N=16) and Melinka (MLK, N=14) (see Figure 1A). The samples from SAU and MIT represent the northern cytoplasmic lineage, the

188 samples from MTM and LEB represent the central cytoplasmic lineage, and the samples
189 from PIL and MLK represent the southern cytoplasmic lineage (Figure 1A). Cytoplasmic
190 markers sequences are not available for all the samples genotyped with microsatellites.
191 However, since the geographic distribution of the three different cytoplasmic clades
192 (Montecinos et al., 2012) was shown to be strictly parapatric (i.e. each region
193 corresponding to a single cytoplasmic clade with no mixture and no overlapping of
194 distribution of haplotypes between regions), geographical origin of the individuals was
195 considered as a good proxy for cytoplasmic clades' assignation. Direct observations of
196 the reproductive organs (tetrads) in the field were used to select only diploid
197 tetrasporophytes in each localities sampled.
198 PCR reactions were performed in 12.5 μL reactions containing 50 ng of template
199 DNA, 1X PCR buffer, 0.2 mM dNTPs, 0.5 μM of each primer and 1 U Top Taq DNA
200 polymerase (Qiagen, Valencia, CA, USA). The concentrations of BSA and $MgCl_2$ are
201 shown in Table S1. The PCR program consisted of an initial denaturation of 3 min at
202 94°C, 35 cycles each with 94°C for 40 s, 40 s at optimized Ta (Table S1), and 30 s at
203 72 °C, and with a final extension of 7 min at 72 °C. PCR products were sent to the
204 Servicio de Secuenciacion Depto. Ecologia, Pontificia Universidad Catolica de Chile,
205 Chile, for fragment analyses. Fragments were separated using an Applied Biosystems
206 3130XL Genetic Analyzer (Life Technologies Corporation).

207 *Statistical analyses* – Allele size was determined with the GENEMARKER software
208 (SoftGenetics, State Collage, PA, USA). Prior to analyses, the frequency of null alleles
209 was estimated for each locus using MICRO-CHECKER (Van Oosterhout et al. 2004;
210 Brookfield equation 2, Brookfield 1996). Linkage disequilibrium at all locus pairs was

211 assessed using FSTAT version 2.9.3.2 (Goudet 2001). Statistical significance of LD was
212 calculated based on 1000 permutations using Bonferonni correction for $\alpha = 0.05$. Single
213 and multilocus estimates of genetic diversity were calculated as the mean number of
214 alleles per locus (*Na*), expected heterozygosity (*He*, sensus Nei 1978) and observed
215 heterozygosity (*Ho*) using GENETIX 4.05 (Belkhir et al. 1996-2004). Allele frequencies
216 were calculated for each study site at each locus and plotted using the R-package
217 StandArich (available at http://www.ualg.pt/ccmar/maree/software.php, F. Alberto,
218 University of Algarve, Faro, Portugal). Single and multilocus estimates of deviation from
219 random mating (F_{IS}) were calculated according to Weir and Cockerham (1984),
220 significance was determined by running 1000 permutations of alleles among individuals
221 within sites using GENETIX 4.05 (Belkhir et al. 1996-2004). Genetic differentiation
222 among sites was analyzed by estimating F_{ST} (θ) (Weir and Cockerham 1984);
223 significance of F_{ST} values was assessed by running 1000 permutations using GENETIX
224 4.05 (Belkhir et al. 1996-2004). Principal component analysis (PCA) was conducted
225 using PCAGEN (Goudet 1999) to visualize pairwise differentiation among sites (F_{ST});
226 1,000 randomizations of genotypes were used to determine axis significance. Bayesian
227 inference was implemented in STRUCTURE v. 2.2 (Pritchard et al. 2000) in order to
228 detect potential signs of hybridization and/or introgression between lineages. We used the
229 admixture model and allowed for correlated allele frequencies between sites. A range of
230 clusters (K), from 1 to 10 were tested. Each run, replicated 20 times, consisted of 400000
231 iterations after a "burn-in" of 200000. To infer which K best fit the data, we applied the
232 ad hoc ΔK statistic developed by Evanno et al. (2005). The results from STRUCTURE
233 were then compared to those of INSTRUCT (Gao et al. 2007), which relaxes

STRUCTURE's assumption of Hardy-Weinberg equilibrium as it was designed for species with significant self-fertilization. INSTRUCT was run with the parameters "-K 3 -v 2 -x 0 -w 0 -j 20000 -e 0 -f 0 -L 9 -N 96 -p 2 -u 600000 -b 200000 -t 10 -c 20 -sl 0.95 -g 1 -r 20000 -ik 1 -kv 1 10 -df 1 -af 0 -mm 2.0e9" with K ranging from 1 to 10 (i.e. –kv). For both STRUCTURE and INSTRUCT analyses, combined results of the independent runs were obtained using the greedy algorithm with100000 random input orders in CLUMMP (Jakobsson and Rosenberg 2007) before exporting the results to DISTRUCT (Rosenberg 2004) for viewing.

Results

We obtained 172872 reads for the northern lineage, 238901 reads for the central lineage and 111945 reads for the southern lineage (average length: 436 bp). In total, 1091 microsatellite inserts were observed for the northern lineage, 1805 for the central lineage and 667 for the southern lineage (see Table S2 for more details). Most of the microsatellites recovered were di- (87.3%) and trinucleotides (10.8%) while larger repeated motifs were rare (0.9% tetranucleotides and 0.9% pentanucleotides) (Table S2).

Of the 12 polymorphic loci developed during this study (Table S1, Table S3), three loci (Ml_39C37, Ml_106C1748 and Ml_106C203) were not retained for population genetic analyses. The locus Ml_39C37 was not retained because it presented strong and significant linkage disequilibrium with locus Ml_106C32. The locus Ml_106C1748 failed to amplify in 33 of the 96 DNA samples (NI/n = 0.6, Table S3) and the locus Ml_106C203 presented a very low level of polymorphism. Indeed, Ml_106C203 was

256 fixed for all sites from the northern and southern lineage and only two alleles were
257 observed over the whole dataset (Table S3).

258 For the nine loci selected (i.e. shaded in grey in Table S3), observed
259 heterozygosities ranged from 0.11 to 0.57 while expected heterozygosities ranged from
260 0.59 to 0.87 for the whole data set (Table S3). The number of alleles encountered in each
261 site varied from 1 to 10 while the average number of alleles per locus was 3.11 (SE =
262 1.69) (Table S3). Three loci were moderately polymorphic (4–6 alleles) and six were
263 highly variable (9–26 alleles). The frequency of null alleles was significant for five loci
264 in some of the sites studied (Ml_106C75 in four sites; Ml_106C32 in two sites; and
265 Ml_39C1451, Ml_39C5118 and Ml_39C4313 in only one site) (Table S3). The estimated
266 frequency of null alleles ranged from 0.12 to 0.36 (Table S3).

267 F_{IS} values were highly variable among loci and sites. The number of significant
268 F_{IS} values per locus was only slightly higher in the central lineage (8/16) than in the
269 northern (6/15) and southern lineages (6/17) (Table S3). However, the F_{IS} multilocus
270 estimates (Table 1) show that only LEB and PIL were close to panmixia (F_{IS} = -0.03 and
271 -0.07, respectively). Alternatively, a negative and significant F_{IS} was encountered for
272 MLK (F_{IS} = -0.17), and positive and significant F_{IS} values were encountered in the three
273 northern most sites of SAU, MIT and MTM (F_{IS} = 0.16, 0.14 and 0.45, respectively,
274 Table 1). Similar results were obtained when corrections for null alleles were made
275 (Table 1).

276 Allele size distributions generally overlapped between cytoplasmic lineages when
277 all six sites were taken into account (Figure S1). However, for three of the 12 loci
278 (Ml_106_C462, Ml_39_C69 and Ml_106_C32, Figure S1), allele distributions were

totally disjoint between the southernmost and northernmost cytoplasmic clades (i.e. these three loci are diagnostic for each of the two clades). In addition, a clear gradient of variation in allele size with respect to latitude was observed for those three loci (Figure S1). For the loci Ml_39C69 and Ml_106C462, shorter alleles were encountered in sites from the northern lineage while for the locus Ml_106C32 shorter alleles were observed in sites from the southern lineage (Figure S1). Sites belonging to the central lineage had alleles of intermediate size; the MTM site presented allele sizes that were more similar to the northern lineage while the LEB site presented allele sizes was more similar to the southern lineage (Figure S1). For the Ml_106_C462, Ml_39_C69 and Ml_106_C32 loci, the LEB site presented 27.3% of private alleles, 54.5% of alleles that were shared with the two sites representing the southern cytoplasmic clade (PIL and MLK) and 9.1% of alleles that were shared with the two sites representing the northern cytoplasmic clade (SAU and MIT) (Figure S1). For the same three loci, the MTM site presented 76.9% of private alleles, 7.7% of alleles that were shared with the two sites representing the southern cytoplasmic clade and 23.1% of alleles that were shared with the two sites representing the northern cytoplasmic clade (Figure S1).

The PCA summarized the information given by the nine loci (Figure 1B) and showed results that were congruent with the allele size distribution results. The first two axes explained 39.4% (PC1) and 26.0% (PC2) of the total genetic differentiation (F_{ST}) (Figure 1B). The first axis separated sites of the northern lineage (SAU and MIT) from all other lineages (MTM, LEB, PIL and MLK) while the second axis discriminated sites of the central lineage from those of the southern lineage (Figure 1B). However, the MTM site holds a unique position in the PCA and was located in-between the group composed

302 of the three southernmost sites (LEB, PIL and MLK) and the two sites from the northern
303 lineage along the first axis and was separated from the other five study sites along the
304 second axis (Figure 1B). All pairwise F_{ST} multilocus values were significantly different
305 from zero and ranged from 0.253 (between PIL and MLK, both from the southern
306 lineage) to 0.581 (between PIL and SAU, northern vs southern lineage differentiation,
307 Table S4). Similar results were found when using the dataset after corrections for null
308 alleles were made (pairwise F_{ST} ranges from 0.249 to 0.572, Table S4).

309 Results from the clustering analysis performed with both STRUCTURE and
310 INSTRUCT, revealed that the posterior probability of the data increased steadily from K
311 = 1 to K = 6 while the curves dropped after K = 7 (Figure S2 and S3). The ΔK method of
312 Evanno et al. (Evanno et al. 2005) clearly shows that both K2 and K6 clusters are the
313 optimal numbers of clusters in our study (Figure S2). Contrary to our expectations, the
314 number of nuclear genetic clusters retrieved was two or even six but definitely not three
315 as predicted with organelle sequences. For K=6, both STRUCTURE and INSTRUCT
316 identified the same 6 clusters each corresponding to a different sampling site
317 (STRUCTURE: Figure 2; INSTRUCT: Figure S3). Almost all individuals from the same
318 site had similar membership coefficients and, overall, a very low level of admixture was
319 observed (Figure 2, K6 and Figure S3). This result indicated that differentiation occurs
320 between all of the sampling sites. The Bayesian clustering assignment in STRUCTURE
321 for K = 2 shows that all individuals from the northern lineage (i.e. SAU and MIT)
322 grouped together while the three southernmost sites belonging to the central and southern
323 lineages (i.e. LEB, PIL and MLK) formed another cluster. However, clustering of the
324 MTM individuals to one or the other cluster did vary among the different STRUCTURE

runs. Eleven of the 20 runs (Figure 2, K2 upper graph) assigned all MTM individuals to the northern genetic cluster while individuals from MTM were assigned to the southern genetic cluster for the other 9 runs (Figure 2, K2 lower graph). Only central lineage cytoplasmic COI sequences were observed (M-L. Guillemin, unpublished data) in this site located only 13 kilometres from the contact zone with the northern lineage (Figure 1A).

Discussion

In this study, nine variable microsatellite markers have been developed for *M. laminarioides* using 454 next-generation sequencing. Recently, this method has been used successfully to develop microsatellite markers for various eukaryotic species (see the review by Meglécz et al. 2012) including some red algae (Couceiro et al. 2011a, Pardo et al. 2014, Ayres-Ostrock et al. 2015). Repetitive sequences were encountered in less than 0.7% of the *M. laminarioides* reads. In other red algae (Couceiro et al. 2011a, Pardo et al. 2014, Ayres-Ostrock et al. 2015) and in corrals (Ruiz-Ramos and Baums 2014), the percentage of repetitive sequences is generally much higher and ranges from 1.3% in the candelabrum coral *Eunicea flexuosa* to 11.6% in the coralline alga *Phymatolithon calcareum*. This scarcity of repetitive sequences clearly reduced our capacity to develop microsatellites markers for *M. laminarioides* where less than 0.03% of the reads yielded microsatellites with sufficient motif repetitions (i.e. >7). Considering that the main aim of this study was to investigate the pattern of gene flow across the 33°S and the 38°S transition zones, only loci that amplified in all three lineages were selected. A reported drawback of cross-amplifying loci is the high probability of generating an

348 uneven amplification of the target loci, which could result from defective primers or
349 deviations from optimal amplification conditions, between different taxa (Selkoe and
350 Toonen 2006). In our study, five loci revealed a moderate to high frequency of null
351 alleles in some sites. In *M. laminarioides*, no clear differences were observed between the
352 F_{IS} and the F_{ST} estimates calculated using the uncorrected or corrected datasets. As such,
353 the F_{IS} and F_{ST} values obtained in our study, even if null alleles are potentially present,
354 can be used to infer biological processes in this species.

355 The results found here only partially supported the previously defined *M.*
356 *laminarioides* lineages based on cytoplasmic markers (Montecinos et al. 2012). Indeed,
357 contrary to our expectations, the number of main nuclear genetic clusters retrieved by
358 STRUCTURE was two and not three as predicted with organelle sequences. Based on the
359 nuclear marker data, the two northernmost sites (SAU and MIT) that correspond to the
360 northern cytoplasmic lineage and the two southernmost sites (PIL and MLK) that
361 correspond to the southern cytoplasmic lineage formed two differentiated groups. The
362 presence of several unique, high frequency diagnostic alleles supports the existence of a
363 long-term divergence between these two lineages. On the other hand and contrary to the
364 previous results found using cytoplasmic markers (Montecinos et al. 2012), the sites from
365 the central cytoplasmic lineage (MTM and LEB) do not represent a third well-separated
366 group according to nuclear microsatellites. While LEB clearly grouped with sites of the
367 southern cytoplasmic lineage, the position of MTM stays unclear. Indeed, MTM appeared
368 highly differentiated from the other five sites sampled in the PCA. However, shared
369 alleles with sites that correspond to both the northern and southern cytoplasmic lineages
370 were observed in MTM and the site was not assigned to a third main nuclear genetic

371 cluster in the STRUCTURE analyses but actually shifted between the northern and the
372 southern genetic cluster, depending on the STRUCTURE run for K2. The discordance
373 observed between the present study, based on nuclear markers, and the previously
374 published work based on cytoplasmic markers could simply be explained by incomplete
375 lineage sorting of the nuclear genes. Due to the differences in effective population size
376 between the maternally and the bi-parentally inherited genomes (nuclear effective
377 population size is approximately four times greater than that of the mitochondria and
378 chloroplast) lineage sorting is expected to be faster for organelle genomes than for the
379 nucleus. It is thus expected to observe greater genetic differentiation using mtDNA and
380 cpDNA genes than when using nuclear genes (see Zink and Barrowclough 2008 for a
381 review). Discordance between genomes can also arise if there are differences in the way
382 selection acts on the non-recombinant cytoplasmic genomes as compared to the nuclear
383 genome; or when past and / or present gene flow took / takes place between lineages
384 (Toews and Brelsford 2012). In their study, Montecinos et al. (2012) recognized that
385 cytoplasmic markers showed shallower divergence between the central and southern
386 linages than between the northern lineage and the central/southern clade. Accordingly,
387 complete reproductive barriers may not have yet evolved between the more recently
388 diverging central and southern linages; this suggests that contemporary gene flow might
389 still connect the three southernmost sites of LEB, PIL, and MLK. Moreover, asymmetric
390 introgressive hybridization in the past could also have lead to the incongruence pattern
391 observed in LEB. In algae, such nuclear / cytoplasmic incongruences were observed in
392 various species and interpreted as footprints of hybridization (Destombe et al. 2010,
393 Hoarau et al. 2015) or past introgression (Neiva et al. 2010, Hoarau et al. 2015). In

394 contrast, the pattern observed for MTM, the other central cytoplasmic lineage site, does
395 not fit this hypothesis of asymmetric introgression. MTM was highly differentiated from
396 both the northern sites (SAU and MIT, ~ 230 km away, $F_{ST} > 0.5$) and the central and
397 southern sites (LEB, PIL and MLK, ~ 550 km away, $F_{ST} > 0.4$). Individuals from this site
398 exhibited a high number of private alleles with intermediate sizes between the sizes of the
399 diagnostic alleles of the two nuclear groups. The MTM site is located only 13 kilometers
400 away from the contact zone with the northern lineage. However, only one individual of
401 MTM was determined to be a possible hybrid. This individual correspond to a genotype
402 assigned mostly to the MTM cluster but for which the secondary cluster of MIT
403 represents more than 5% of the genome in both the STRUCTURE and the INSTRUCT
404 clustering results for K6 (see Figure 2 and S3). The genetic composition of this individual
405 was more consistent with an old hybridization event followed by consecutive backcrosses
406 than with a recent hybridization event. This result reinforce the idea that gene leakage is
407 reduced even at the 33°S transition zone margin.

408 It is hypothesized that progressive, multiple genome-wide changes accumulated
409 by drift or selection between two gene pools will lead to the build-up of reproductive
410 isolation over time (Nosil and Feder 2012). Hybridization and introgression between two
411 diverging taxa should then diminish with time of divergence. At first sight, this supports
412 the idea that, while reaching a determined threshold of genetic distance, all taxa in a
413 taxonomic group will reach complete reproductive isolation and could then be recognized
414 as a biological species. The existence of such a correlation is the key argument provided
415 to support the creation of a universal threshold to define species using DNA barcoding
416 methods (the 1% threshold for the COI mitochondrial marker as mentioned in BOLD,

417 Ratnasingham and Hebert 2007). However, the timeframe of speciation is strongly
418 influenced by factors such as drift, opportunities for ecological adaptation, and intrinsic
419 rates of mutations (Sobel et al., 2010), and these factors have been shown to vary
420 depending on the taxa being studied (Dufresnes et al. 2014 and 2015). For COI in red
421 algae, genetic distances between 4.5 to 13.6% were reported between species of the same
422 genus (Saunders 2005, Clarkston and Saunders 2010) but sister species of *Mazzaella* that
423 diverged by less than 1.2% were also reported (Saunders 2005). In *M. laminarioides*, the
424 genetic distance between the three COI-defined cytoplasmic lineages were well within
425 the red algae threshold to delimit species in this genus (2.6 to 7.8%, Montecinos et al.
426 2012). Our work shows that, although substantial mtDNA and cpDNA differentiation
427 occurs within *M. laminarioides* (Montecinos et al. 2012), this does not necessarily
428 correlate with the existence of complete reproductive isolation. In this study, as in others
429 focused on recently diverging lineages distributed in parapatry (Colliard et al. 2010,
430 Zarza 2011, Dufresnes et al. 2014 and 2015), cytoplasmic markers and microsatellites did
431 not reveal the same pattern of genetic subdivision. However, due to the low number of
432 sites sampled in our study, the true number of *M. laminarioides* nuclear genetic groups
433 will remain unresolved until a more detailed sampling is conducted.

434 The very high F_{ST} estimates (all > 0.24) obtained in our study suggest that gene
435 flow between the sampled sites is minimal even when sites were previously classified as
436 part of the same nuclear genetic group and cytoplasmic lineage. The retrieval of six
437 clusters, each corresponding to a different sampling site and showing a very low level of
438 admixture, by both STRUCTURE and INSTRUCT, confirm the high differentiation
439 between our six sampling sites. Red algae, that lack long-lived motile gametes, spores,

440 and floating structures, are ranked among the poorest dispersers when compared to other
441 marine taxa (Kinlan and Gaines 2003). Genetic differentiation has been reported at the
442 scale of kilometres or even meters in these organisms (Faugeron et al. 2001, Zuccarello et
443 al. 2001, Engel et al. 2004, Couceiro et al. 2011b, Krueger-Hadfield et al. 2013). As
444 reported for *M. laminarioides* by Faugeron et al. (2001) using random amplified
445 polymorphic DNA (RAPD) markers, high and significant genetic structure exists
446 between sites located less than 40km apart (F_{ST} = 0.39 between SAU and MIT). F_{ST}
447 estimates between the three southernmost sites (LEB, PIL and MLK), spanning more
448 than 730km of coast, were significant but lower ($0.24 < F_{ST} < 0.35$) than estimates
449 calculated for the northern sites. Interestingly, the same pattern was reported for the
450 cytoplasmic markers (Montecinos et al. 2012) where genetic structure was much more
451 pronounced in the northern lineage than in the southern lineage. The authors associated
452 the attributed differences between the northern and southern groups to historical
453 demographic differences. They concluded that southern populations of *M. laminarioides*
454 were strongly affected by Quaternary glaciations that would have caused recent
455 demographic expansion while northern populations would have experienced repeated
456 local extinctions and range fragmentations due to the El Niño Southern Oscillation
457 (ENSO) (Montecinos et al. 2012).

458 These regional differences between the north and the south could also explain the
459 marked differences between the F_{IS} estimates reported in our study. Highly significant
460 heterozygote deficiencies were observed in the three northernmost site of SAU, MIT and
461 MTM while the sites of LEB and PIL had observed heterozygosities close to random
462 mating. Departure from random mating in the north could be explained by the recurrence

463 of massive mortality due to ENSO events observed in this region; this would have
464 resulted in patches of small fragmented populations (as reported in algae, Martínez et al.
465 2003). In the site of MTM, located at the edge of the contact zone with the highly
466 divergent northern lineage (Montecinos et al. 2012), selfing (intergametophytic selfing,
467 see Krueger-Hadfield et al. 2015) could limit gene flow and protect parental genotypes
468 from the formation of hybrid progeny (Antonovics 1968). The prominent role of selfing
469 in the emergence of reproductive barriers has been observed in plants (Martin and Willis
470 2007, Matallana et al. 2010), fungi (Gibson et al. 2011) and brown algae (Engel et al.
471 2005, Billard et al. 2010, Hoarau et al. 2015). Small scale sampling within the 33°S
472 contact zone is needed to both determine the exact role of selfing as a reinforcement
473 mechanism in *M. laminarioides* and to better characterize the possible mechanisms
474 responsible of the onset and progress of divergence between the northern and
475 central/south lineages.

476 In conclusion, this study revealed discordant pattern of geographic variation
477 between nuclear microsatellite markers and cytoplasmic sequences in the red alga
478 *Mazzaella laminarioides*. The presence of several diagnostic alleles did support the
479 existence of a long-term divergence between the northernmost and southernmost
480 cytoplasmic lineages. However, the central cytoplasmic lineage did not form a third
481 nuclear independent group and a high number of shared alleles are observed, principally
482 with the southern cytoplasmic lineage. This shared polymorphism may be explained
483 either by retention of ancestral polymorphism or by hyridization between cytoplasmic
484 lineages. The likelihood of shared ancestral polymorphism vs. recurrent gene flow in
485 these closely related parapatric lineages is a question difficult to test but that we cannot

resolve. Indeed, our study reveals intriguing results for the two sites of the central lineage and jointly leads us to ask if MTM (located at the northern limit of the central lineage) could represent a third nuclear group while the pattern observed in LEB (located in the southern part of the central lineage distribution) is mostly due to ancient or recent gene flow with the neighboring southern lineage. A much denser sampling, especially between the 33°S and the 38°S where the central lineage is located, is needed to better characterize the complex genetic pattern observed in this region. The southern part of the 33-38°S coast forms a mosaic of sandy beaches and rocky coast characterized by rapid changes due to high tectonic activity. Processes, linked to extinction and recolonization, have probably shaped the intertidal algae population of this region leading to complex pattern of genetic differentiation. Nuclear microsatellites clearly show that *M. laminarioides* does not correspond to a single species widely distributed over 3,500km of Chilean coast. These markers rather suggest that one or several speciation processes have probably shaped the present-day patterns of genetic diversity in this species complex. Unraveling the relations between the *M. laminarioides* taxa should be the goal of future works.

Acknowledgements

This research was supported by FONDECYT N°1130797 (CONICYT, Comisión Nacional de Investigación Científica y Tecnológica, Gobierno de Chile). The authors thank S. Faugeron for the access to *Mazzaella laminarioides* DNA for the 454-library construction. Additional support came from the International Research Network

508 ‘‘Diversity, Evolution and Biotechnology of Marine Algae’’ (GDRI N˚0803). The
509 authors have declared that no competing interests exist.
510
511
512 Bibliography
513 Ahn, S. J., Costa, J. & Emanuel, J. R. 1996. PicoGreen quantitation of DNA:
514 effective evaluation of samples Pre-or post-PCR. *Nucleic acids res.* 24(13):2623–2625.
515 Ayres-Ostrock, L. M., Mauger, S., Plastino, E. M., Oliveira, M. C., Valero, M. &
516 Destombe, C. 2015. Development and characterization of microsatellite markers in two
517 agarophyte species, *Gracilaria birdiae* and *Gracilaria caudata* (Gracilariaceae,
518 Rhodophyta), using next-generation sequencing. *J. Appl. Phycol.* 1–10.
519 Belkhir, K., Borsa, P., Chikhi, L., Raufaste, N. & Bonhomme, F. 1996-2004.
520 Genetix 4.02, Logiciel Sous Windows TM Pour La Génétique Des Populations.
521 Laboratoire Génome, Populations, Interactions, CNRS UMR. 5000, Université de
522 Montpellier II, Montpellier.
523 Billard, E., Serrão, E., Pearson, G., Destombe, C. & Valero, M. 2010. *Fucus*
524 *vesiculosus* and *spiralis* species complex: a nested model of local adaptation at the shore
525 level. *Mar. Ecol. Prog. Ser*. 405:163–174.
526 Brodie, J. & Zuccarello, G. C. 2006. Systematics of the species rich algae: red
527 algal classification, phylogeny and speciation. *In* Hodkinson, T. R. & Parnell, J. A. N.
528 [Eds.] *Reconstructing the Tree of Life: Taxonomy and Systematics of Species Rich Taxa*.
529 The Systematics Associations, Boca Raton, Florida, pp.317–30.
530 Buschmann, A. H., Correa, J. A., Westernmeier, E., Hernandez- Gonzalez, M. D.

C. & Normabuena, R. 2001. Red algal farming in Chile: a review. *Aquaculture* 194:203–220.

Brookfield, J. F. Y. 1996. A simple new method for estimating null allele frequency from heterozygote deficiency. *Mol. Ecol.* 5:453–455.

Camus, P. A. 2001. Biogeografía marina de Chile continental. *Rev. Chil. Hist. Nat.* 74(3):587–617.

Chevreux, B., Wetter, T. & Suhai, S. 1999. Genome sequence assembly using trace signals and additional sequence information. *Compt. Sci. Biol. Proc. Ger. Conf. Bioinformatics* 99:45–56.

Clarkston, B. E. & Saunders, G. W. 2010. A comparison of two DNA barcode markers for species discrimination in the red algal family Kallymeniaceae (Gigartinales, Florideophyceae), with a description of *Euthora timburtonii* sp. nov. *Botany* 88(2):119–131.

Colliard, C., Sicilia, A., Turrisi, G. F., Arculeo, M., Perrin, N. & Stöck, M. 2010. Strong reproductive barriers in a narrow hybrid zone of West-Mediterranean green toads (*Bufo viridis* subgroup) with Plio-Pleistocene divergence. *BMC Evol. Biol.* 10(1):232.

Couceiro, L., Maneiro, I., Mauger, S., Valero, M., Ruiz, J. M. & Barreiro, R. 2011a. Microsatellite development in Rhodophyta using high‐throughput sequence data. *J. Phycol.* 47(6):1258–1265.

Couceiro, L., Maneiro, I., Ruiz, J. M. & Barreiro, R. 2011b. Multiscale genetic structure of an endangered seaweed *Ahnfeltiopsis pusilla* (Rhodophyta): implications for its conservation. *J. Phycol.* 47(2):259–268.

Destombe, C., Valero, M. & Guillemin, M-L. 2010. Delineation of two sibling red

554 algal species, *Gracilaria gracilis* and *Gracilaria dura* (Gracilariales, Rhodophyta), using
555 multiple DNA markers: resurrection of the species *G. dura* previously described in the
556 northern Atlantic 200 years ago. *J. Phycol.* 46:720–7.
557 Dufresnes, C., Bonato, L., Novarini, N., Betto-Colliard, C., Perrin, N., & Stöck,
558 M. 2014. Inferring the degree of incipient speciation in secondary contact zones of
559 closely related lineages of Palearctic green toads (*Bufo viridis* subgroup). *Heredity*
560 113(1):9–20.
561 Dufresnes, C., Brelsford, A., Crnobrnja-Isailović, J., Tzankov, N., Lymberakis, P.
562 & Perrin, N. 2015. Timeframe of speciation inferred from secondary contact zones in the
563 European tree frog radiation (*Hyla arborea* group). *BMC Evol. Biol.* 15(1):155.
564 Engel, C. R., Daguin, C. & Serrão, E. A. 2005. Genetic entities and mating system
565 in hermaphroditic *Fucus spiralis* and its close dioecious relative *F. vesiculosus* (Fucaceae,
566 Phaeophyceae). *Mol. Ecol*. 14:2033–2046.
567 Engel, C. R., Destombe, C. & Valero, M. 2004. Mating system and gene flow in
568 the red seaweed *Gracilaria gracilis*: effect of haploid-diploid life history and intertidal
569 rocky shore landscape on finescale genetic structure. *Heredity* 92:289–298.
570 Evanno, G., Regnaut, S. & Goudet, J. 2005. Detecting the number of clusters of
571 individuals using the software STRUCTURE: a simulation study. *Mol. Ecol*.14:2611–
572 2620.
573 Faircloth, B. C. 2008. MSATCOMMANDER: detection of microsatellite repeat
574 arrays and automated, locus-specific primer design. *Mol. Ecol. Res*. 8:92–94.
575 Faugeron S., Valero M., Destombe C., Martínez E. A. & Correa, J. A. 2001.
576 Hierarchical spatial structure and discriminant analysis of genetic diversity in the red alga

577 *Mazzaella laminarioides* (Gigartinales, Rhodophyta). *J. Phycol*. 37:705–716.

578 Fraser, C. I., Nikula, R., Spencer, H. G. & Waters, J. M. 2009. Kelp genes reveal
579 effects of subantarctic sea ice during the Last Glacial Maximum. *Proc. Natl. Acad. Sci.*
580 *USA* 106:3249–3253.

581 Fraser, C. I., Zuccarello, G. C., Spencer, H. G., Salvatore, L. C., Garcia, G. R., &
582 Waters, J. M. 2013. Genetic affinities between trans-oceanic populations of non-buoyant
583 macroalgae in the high latitudes of the Southern Hemisphere. *PLoS ONE* 8(7):e69138.

584 Gao, H. S., Williamson, S. & Bustamante, C. D. 2007. A Markov chain Monte
585 Carlo approach for joint inference of population structure and inbreeding rates from
586 multilocus genotype data. *Genetics* 176:1635–1651.

587 Gibson, A. K., Hood, M. E. & Giraud, T. 2012. Sibling competition arena: selfing
588 and a competition arena can combine to constitute a barrier to gene flow in sympatry.
589 *Evolution 66*(6):1917–1930.

590 Goudet, J. 1999. [http://www2.unil.ch/popgen/softwares/pcagen.htm].

591 Goudet, J. 2001. FSTAT, a program to estimate and test gene diversities and
592 fixation indices (version 2.9. 3).

593 Guillemin, M-L., Valero, M., Tellier, F., Macaya, E. C., Destombe, C. &
594 Faugeron, S. 2015. Phylogeography of seaweeds in the South East Pacific: complex
595 evolutionary processes along a latitudinal gradient. *In* Hu Z-M. & Fraser, C. [Eds.]
596 *Seaweed phylogeography.* Springer Verlag, Berlin.

597 Hoarau, G., Coyer, J. A., Giesbers, M. C. W. G., Jueterbock, A., & Olsen, J. L.
598 2015. Pre-zygotic isolation in the macroalgal genus *Fucus* from four contact zones
599 spanning 100–10 000 years: a tale of reinforcement? *Royal Society Open Science*

600 2(2):140538.
601 Huang, X. Q. & Madan, A. 1999. CAP3: a DNA sequence assembly program.
602 *Genome Res*. 9:868–877.
603 Jakobsson, M. & Rosenberg, N. A. 2007. CLUMPP: a cluster matching and
604 permutation program for dealing with label switching and multimodality in analysis of
605 population structure. *Bioinformatics* 23(14):1801–1806.
606 Kinlan, B. P. & Gaines, S. D. 2003. Propagule dispersal in marine and terrestrial
607 environments: a community perspective. *Ecology* 84:2007–20.
608 Krueger-Hadfield, S. A., Roze, D., Correa, J. A., Destombe, C. & Valero, M.
609 2015. O father where art thou? Paternity analyses in a natural population of the haploid-
610 diploid seaweed *Chondrus crispus*. *Heredity* 114:185–194.
611 Krueger-Hadfield, S. A., Roze, D., Mauger, S. & Valero, M. 2013.
612 Intergametophytic selfing and microgeographic genetic structure shape populations of the
613 intertidal red seaweed *Chondrus crispus*. *Mol. Ecol.* 22(12):3242–3260.
614 Lindstrom, S. C., Gabrielson, P. W., Hughey, J. R., Macaya, E. C., & Nelson, W.
615 A. 2015. Sequencing of historic and modern specimens reveals cryptic diversity in
616 *Nothogenia* (Scinaiaceae, Rhodophyta). Phycologia 54 (2):97–108.
617 Mackay, J. F., Wright, C. D. & Bonfiglioli, R. G. 2008. A new approach to
618 varietal identification in plants by microsatellite high resolution melting analysis:
619 application to the verification of grapevine and olive cultivars. *Plant Methods* 4(1):8.
620 Matallana, G., Godinho, M. A. S., Guilherme, F. A. G., Belisario, M., Coser, T. S.
621 & Wendt, T. 2010. Breeding systems of Bromeliaceae species: evolution of selfing in the
622 context of sympatric occurrence. *Plant. Syst. Evol*. 289:57–65.

623 Martin, N. H., & Willis, J. H. 2007. Ecological divergence associated with mating
624 system causes nearly complete reproductive isolation between sympatric *Mimulus species*.
625 *Evolution* 61:68–82.
626 Martínez, E. A., Cárdenas, L. & Pinto, R. 2003. Recovery and genetic diversity of
627 the intertidal kelp *Lessonia nigrescens* (phaeophyceae) 20 years after el Niño 1982/83. *J.*
628 *Phycol.* 39(3):504–508.
629 Meglécz, E., Nève, G., Biffin, E. & Gardner, M. G. 2012. Breakdown of
630 phylogenetic signal: a survey of microsatellite densities in 454 shotgun sequences from
631 154 non model eukaryote species. *PLoS One 7*(7):e40861.
632 Montecinos, A., Broitman, B. R., Faugeron, S., Haye, P. A., Tellier, F. &
633 Guillemin, M. L. 2012. Species replacement along a linear coastal habitat:
634 phylogeography and speciation in the red alga *Mazzaella laminarioides* along the south
635 east pacific. *BMC Evol. Biol.* 12(1):97.
636 Nei, M. 1978. Estimation of average heterozygosity and genetic distance from a
637 small number of individuals. *Genetics* 89(3):583–590.
638 Neiva, J., Pearson, G. A., Valero, M. & Serrao, E. A. 2010. Surfing the wave on a
639 borrowed board: range expansion and spread of introgressed organellar genomes in the
640 seaweed *Fucus ceranoides* L. *Mol. Ecol.* 19(21):4812–4822.
641 Nosil, P., & Feder, J. L. 2012. Genomic divergence during speciation: causes and
642 consequences. *Philos. T. Roy. Soc. B* 367(1587):332–342.
643 Pardo, C., Peña, V., Bárbara, I., Valero, M. & Barreiro, R. 2014. Development
644 and multiplexing of the first microsatellite markers in a coralline red alga (*Phymatolithon*
645 *calcareum*, Rhodophyta). *Phycologia* 53(5):474–479.

646 Pritchard, J. K., Stephens, M. & Donnelly, P. 2000. Inference of population
647 structure using multilocus genotype data. *Genetics* 155:945–959.
648 Ratnasingham, S. & Hebert, P. D. 2007. BOLD: The Barcode of Life Data System
649 (http://www. barcodinglife. org). *Mol. Ecol. Notes* 7(3):355–364.
650 Rosenberg, N. A. 2004. DISTRUCT: a program for the graphical display of
651 population structure. *Mol. Ecol. Notes* 4(1):137–138.
652 Ruiz-Ramos, D. V. & Baums, I. B. 2014. Microsatellite abundance across the
653 Anthozoa and Hydrozoa in the phylum Cnidaria. *BMC genomics* 15(1):939.
654 Saunders, G. W. 2005. Applying DNA barcoding to red macroalgae: a
655 preliminary appraisal holds promise for future applications. *Philos. T. Roy. Soc. B*
656 360(1462):1879–1888.
657 Selkoe, K. A. & Toonen, R. J. 2006. Microsatellites for ecologists: a practical
658 guide to using and evaluating microsatellite markers. *Ecol. Lett.* 9(5):615–629.
659 Sobel, J. M., Chen, G. F., Watt, L. R. & Schemske, D. W. 2010. The biology of
660 speciation. *Evolution* 64(2):295–315.
661 Tellier, F., Meynard, A. P., Correa, J. A., Faugeron, S., & Valero, M. 2009.
662 Phylogeographic analyses of the 30°S south-east Pacific biogeographic transition zone
663 establish the occurrence of a sharp genetic discontinuity in the kelp *Lessonia nigrescens*:
664 Vicariance or parapatry? *Mol. Phyl. Evol.* 53(3):679–693.
665 Tellier, F., Tapia, J., Faugeron, S., Destombe, C. & Valero, M. 2011. The
666 *Lessonia nigrescens* species complex (Laminariales, Phaeophyceae) shows strict
667 parapatry and complete reproductive isolation in a secondary contact zone. *J. Phycol*.
668 47:894–903.

669 Thiel, M., Macaya, E. C., Acuña, E., Arntz, W. E., Bastias, H., Brokordt, K.,
670 Camus, P. A., Castilla, J. C., Castro, L. R., Cortés, M. et al. 2007. The Humboldt Current
671 System of northern and central Chile. *Oceanogr. Mar. Biol*. 45:195–344.
672 Toews, D. P. & Brelsford, A. 2012. The biogeography of mitochondrial and
673 nuclear discordance in animals. *Mol. Ecol.* 21(16):3907–3930.
674 Van Oosterhout, C., Hutchinson, W. F., Wills, D. P. & Shipley, P. 2004.
675 MICRO‐CHECKER: software for identifying and correcting genotyping errors in
676 microsatellite data. *Mol. Ecol. Notes* 4(3):535–538.
677 Weir, B. S. & Cockerham, C. C. 1984. Estimating F-statistics for the analysis of
678 population structure. *Evolution* 38:1358–1370.
679 Zakas, C., Binford, J., Navarrete, S. A., & Wares, J. P. 2009. Restricted gene flow
680 in Chilean barnacles reflects an oceanographic and biogeographic transition zone. *Mar.*
681 *Ecol. Prog. Ser.* 394:165–177.
682 Zakas, C., Jones, K., & Wares, J. P. 2014. Homogeneous nuclear background for
683 mitochondrial cline in northern range of *Notochthamalus scabrosus*. *G3: Genes Genomes*
684 *Genetics* 4(2):225–230.
685 Zarza, E., Reynoso, V. H. & Emerson, B. C. 2011. Discordant patterns of
686 geographic variation between mitochondrial and microsatellite markers in the Mexican
687 black iguana (*Ctenosaura pectinata*) in a contact zone. *J. Biogeo.* 38(7):1394–1405.
688 Zink, R. M. & Barrowclough, G. F. 2008. Mitochondrial DNA under siege in
689 avian phylogeography. *Mol. Ecol.* 17(9):2107–2121.
690 Zuccarello, G. C., Schidlo, N., Mc Ivor, L. & Guiry, M. D. 2005. A molecular re-
691 examination of speciation in the intertidal red alga *Mastocarpus stellatus* (Gigartinales,

692 Rhodophyta) in Europe. *Eur. J. Phycol.* 40:337–44.
693 Zuccarello, G. C. & West, J. A. 2002. Phylogeography of the *Bostrychia*
694 *calliptera-B. pinnata* complex (Rhodomelaceae, Rhodophyta) and divergence rates based
695 on nuclear, mitochondrial and plastid DNA markers. *Phycologia* 41(1):49–60.
696 Zuccarello, G. C. & West, J. A. 2003. Multiple cryptic species: molecular
697 diversity and reproductive isolation in the *Bostrychia radicans/B. moritziana* complex
698 (Rhodomelaceae, Rhodophyta) with focus on North American isolates. *J. Phycol*.
699 39:948–959.
700 Zuccarello, G. C. & West, J. A. 2011. Insights into evolution and speciation in the
701 red alga *Bostrychia*: 15 years of research. *Algae* 26(1):21–32.
702 Zuccarello, G. C., Yeates, P. H., Wright, J. T. & Bartlett, J. 2001. Population
703 structure and physiological differentiation of haplotypes of *Caloglossa leprieurii*
704 (Rhodophyta) in a mangrove intertidal zone. *J. Phycol*. 37:235–44.
705
706
707

Figure 1: Geographic location of the study sites and cytoplasmic clades along the Chilean coast (A) and principal component analysis (PCA) based on mean pairwise F_{ST} averaged over the nine selected loci (B). In the map, brackets show the cytoplasmic lineages of *M. laminarioides*: "north", "center" and "south". Ellipsoids delineating the three cytoplasmic lineages of *Mazzaella laminarioides* in the PCA were drawn for better visualization, but they do not have any statistical support.

Figure 2: Bayesian analysis using STRUCTURE for the six study sites of *Mazzaella laminarioides*. Each vertical bar represents a different individual. Each shade represents the proportion of individual genome assigned to each genetic group and * indicates individuals for which a secondary cluster represents more than 5% of the genome (i.e. admixed individuals). Individuals are ordered from north to south. Results are shown for K2 and K6. For K2, since the 20 independent runs give contrasting results depending on the run, two graphs are presented: one that corresponds to 11 of the 20 runs (upper graph) and the other that corresponds to the remaining 9 of the 20 runs (lower graph).

Table 1: Multilocus estimates of the number of alleles per locus (*Na*), expected heterozygosity (*He*), observed heterozygosity (*Ho*) and F_{IS} calculated for the nine selected microsatellite loci. Significant departure from panmixia was tested by running 1,000 permutations of alleles among individuals within sites using GENETIX 4.05 (Belkhir et al. 1996-2004). F_{IS} values significantly different from zero are shown in bold. Both an uncorrected dataset and a dataset corrected for null alleles (Oosterhout et al. 2004) were used for the calculations. For *Na*, *He* and *Ho,* mean and standard deviation computed over the nine loci are noted.

Geographic origin of sampled sites	Site	*Na*	*He*	*Ho*	F_{IS}	*p*
Uncorrected data set						
Northern cytoplasmic lineage	SAU	3.11 (1.69)	0.30 (0.23)	0.26 (0.26)	**0.16**	**0.0180**
	MIT	3.67 (2.69)	0.46 (0.28)	0.41 (0.30)	**0.14**	**0.0360**
Central cytoplasmic lineage	MTM	3.56 (2.35)	0.37 (0.28)	0.21 (0.23)	**0.45**	**0.0000**
	LEB	3.89 (1.83)	0.48 (0.14)	0.51 (0.32)	-0.03	0.3580
Southern cytoplasmic lineage	PIL	3.11 (1.54)	0.35 (0.22)	0.38 (0.27)	-0.07	0.1230
	MLK	3.22 (1.09)	0.55 (0.07)	0.66 (0.22)	**-0.17**	**0.0110**
Data set corrected for the presence of null alleles						
Northern cytoplasmic lineage	SAU	3.11 (1.69)	0.30 (0.24)	0.27 (0.26)	**0.12**	**0.0450**
	MIT	3.67 (2.69)	0.47 (0.29)	0.42 (0.31)	**0.13**	**0.0180**
Central cytoplasmic lineage	MTM	3.56 (2.35)	0.40 (0.31)	0.24 (0.24)	**0.45**	**0.0000**
	LEB	3.89 (1.83)	0.49 (0.14)	0.54 (0.29)	-0.06	0.2100
Southern cytoplasmic lineage	PIL	3.11 (1.54)	0.35 (0.22)	0.39 (0.27)	-0.08	0.1350
	MLK	3.22 (1.09)	0.55 (0.08)	0.66 (0.22)	**-0.17**	**0.0180**

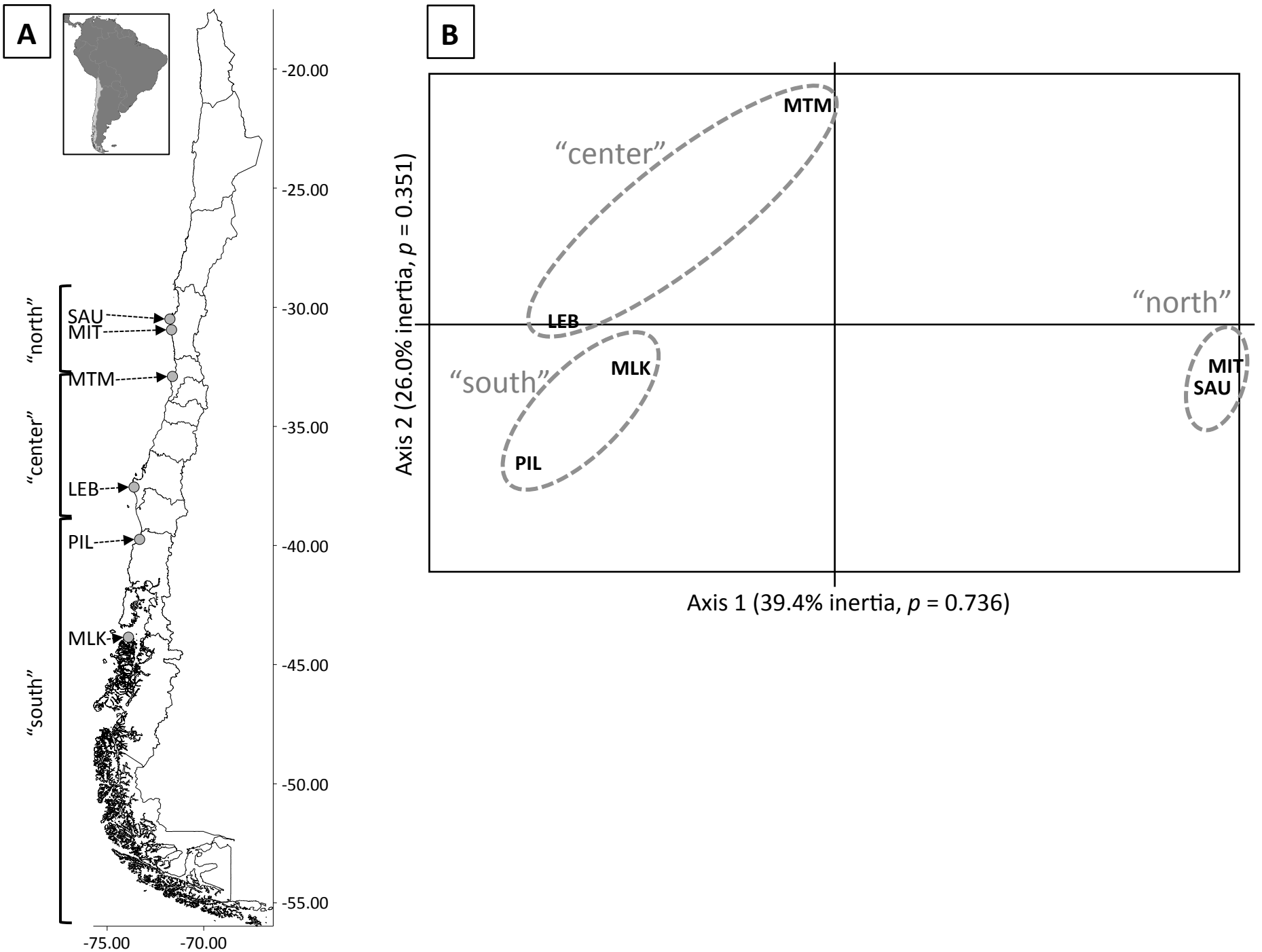
A
-20.00
-25.00
-30.00
-35.00
-40.00
-45.00
-50.00
-55.00
-75.00
-70.00
"north"
"center"
"south"
SAU
MIT
MTM
LEB
PIL
MLK
B
"center"
"north"
"south"
MTM
LEB
MLK
PIL
MIT
SAU
Axis 2 (26.0% inertia, p = 0.351)
Axis 1 (39.4% inertia, p = 0.736)

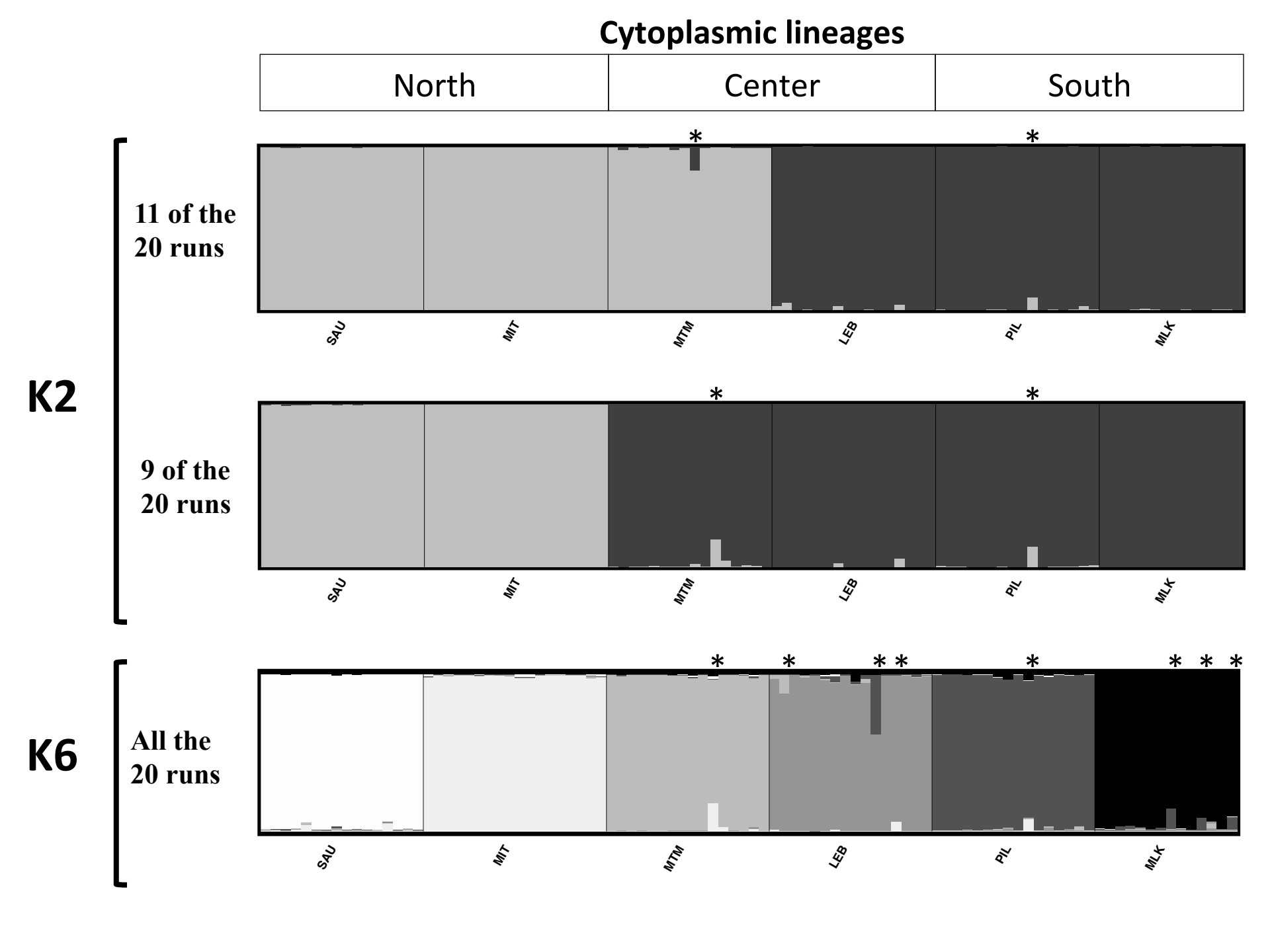
Cytoplasmic lineages
North
Center
South
K2
11 of the 20 runs
9 of the 20 runs
K6
All the 20 runs
SAU
MIT
MTM
LEB
PIL
MLK

Table S1: Characteristics of 12 polymorphic microsatellite loci for the three lineages of *Mazzaella laminarioides*. Repeat motifs are given for every lineage for which the microsatellite sequence was encountered in the 454 nuclear contigs (N = northern lineage, C = central lineage and S = southern lineage). PCR conditions are given for each lineage.

Locus	Primer sequence (5'-3')	Repeat motif[‡]	BSA (µg/µL)	Mg (mM)	Ta (°C)
Ml_106_C462	F: GCAAGGGATGACCATGAC	N: _	0.2	1	62
	R: CTTGTGCCACCTCTATTCTAAGC	C: _	0-0.2*	1-1.5*	62
		S: $(TGA)_{12}$	0	1	62
Ml_106_C10	F: GCGTGTAGCACAGTACTTCTAC	N: $(CA)_{10}AATA(CA)_4$	0	1	65-67*
	R: GAAAGCACCGAAACACAGCC	C: $CATA(CA)_9$	0	1	67
		S: $(CA)_{13}AATA(CA)_4$	0	1	65-67*
Ml_39_C69	F: GCTGTCGAGTGTACGTTTCG	N: _	0.1	1.2	60
	R: GCCTCTGTGAAGCAAGCA	C: $(GA)_9$	0.1	1.2	60
		S: $(GA)_8$	0.1	1.2	60
Ml_106_C75	F: CGCAATCGGGAGCCATCG	N: $(GGCTC)_{12}$	0	0.8	67
	R: CCCTATCGTGTGTTGCCACCG	C: $(GGCTC)_7$	0	0.8	67
		S: $(GGCTC)_5$	0	0.8	65-67*
Ml_106_C32	F: CTGGTACAGTACCGAAGATGTC	N: $(AC)_{12}(ATACACACAC)_6$	0.15	1.2	63-64*
	R: GTTGGGTAATCGAAGAAGATGA	C: $(AC)_{23}ATACTC(AC)_2$	0.15	1.2	63
		S: $(AC)_{13}ATACTC(AC)_2$	0.15	1.2	64
Ml_106_C1748	F: CGTGATGTGTGTCATTTTATCCC	N: $(CCTC)_4N_{44}(TG)_2TA(TG)_2(TGTGTA)_3$	0.2	1	58
	R: CTGTTCCTGTTGTTCCTGCG	C: $(CCTC)_4N_{44}(TG)_2TA(TG)_2GA(TG)_{11}$	0.05	1	61
		S: $(CCTC)_4N_{44}(TG)_2TA(TG)_{11}$	0.05	1	61

Ml_39_C1451	F: GGGAAAAAGCGAGCAATTTG	N: _	0	-	58
	R: CTGTGCCGTCTGACATTG	C: $(TG)_8CG(TG)_4$	0.2	1.5	58
		S: $(TG)_6CG(TG)_4$	0.2	1.5	58
Ml_39_C5118	F: GACTTCGCTGTCCATCCA	N: _	0	-	64
	R: CAACGAATCATCCAGACGAC	C: $(TG)_7TC(TG)_{12}$	0	-	64
		S: _	0	-	64
Ml_106_C203	F: CGGAGGCGACGGAGGAAG	N: $(TG)_5TA(TG)_2CG(TG)_4$	0	1	65
	R: CCTCAATTCCCTCGGTTGCTG	C: $(TG)_8CG(TG)_4$	0	1	66
		S: $((TG)_6CG(TG)_4$	0	1	65
Ml_39_C4313	F: ATCGTTTCAGGGCAATCACTG	N: $(AG)_6(TG)_5$	0	-	56-58*
	R: TCATCCCTCCGTACCTGC	C: $(AG)_6(TG)_6$	0	-	62
		S: $(AG)_6(TG)_5$	0	-	62
Ml_39_C37	F: CGGCGATGATCGACTGAGATAGAA	N: $(TGTGTGTGTA)_5(TG)_{12}$	0.05	1	65
	R: GATGTCCCACCAACGATTGATGG	C: $(TG)_{24}$	0.05	1	65
		S: $(TG)_{14}$	0.05	1	65
Ml_39_C3942	F: CAATGATCGTATTTACTTCGTAGCG	N: $(CGT)_4N_{12}(AT)_5(CT)_2$	0.2	1	59-61*
	R: GCTAACCACAATACTGGCT	C: $(CGT)_4N_{10}(AT)_9C(AT)_2(CT)_3$	0.2	1	61
		S: _	0.2	1	59-61*

Ta annealing temperature for the PCR program.

* When PCR conditions were different between sites from the same lineage, the range of Ta and BSA and Mg2 concentration used are given.

[£] A single haploid (i.e. a female gametophyte) specimen was used as the source of DNA for each three cytoplasmic lineages of *M. laminarioides* to construct the 454 libraries. Samples from Fray Jorge (30°40'S/71°42'W), Constitución (35°19'S/72°26'W) and Chiloe (41°52'S/71°01'W) were used for the northern, central and southern lineage respectively (Montecinos et al. 2012). BLAST searches between the three cytoplasmic lineages contig files were performed to identify microsatellite loci sequenced in more than one of our three 454 libraries (see Material and Methods).

Table S2: Counts of loci for each combination of microsatellite category (di-, tri-, tetra-, and pentanucleotides) and number of perfect tandem repeat units in each *Mazzaella laminarioides* cytoplasmic lineage (i.e. “north”, “center” and “south).

M. laminarioides "north"		N° Rep.	N		N° Rep.	N		N° Rep.	N		N° Rep.	N
	Di	4	791	Tri	4	99	Tetra	4	9	Penta	4	10
	Di	5	113	Tri	5	15	Tetra	5	0	Penta	5	0
	Di	6	22	Tri	6	6	Tetra	6	1	Penta	6	0
	Di	7	10	Tri	7	2	Tetra	7	0	Penta	7	0
	Di	8	3	Tri	8	0	Tetra	8	0	Penta	8	0
	Di	9	0	Tri	9	1	Tetra	9	0	Penta	9	0
	Di	10	2	Tri	10	0	Tetra	10	0	Penta	10	0
	Di	>10	7	Tri	>10	0	Tetra	>10	0	Penta	>10	0

M. laminarioides "center"		N° Rep.	N		N° Rep.	N		N° Rep.	N		N° Rep.	N
	Di	4	1317	Tri	4	129	Tetra	4	10	Penta	4	11
	Di	5	175	Tri	5	35	Tetra	5	3	Penta	5	1
	Di	6	41	Tri	6	11	Tetra	6	0	Penta	6	0
	Di	7	22	Tri	7	1	Tetra	7	1	Penta	7	1
	Di	8	11	Tri	8	4	Tetra	8	0	Penta	8	0
	Di	9	5	Tri	9	8	Tetra	9	0	Penta	9	0
	Di	10	3	Tri	10	0	Tetra	10	0	Penta	10	0
	Di	>10	13	Tri	>10	3	Tetra	>10	0	Penta	>10	0

M. laminarioides "south"		N° Rep.	N		N° Rep.	N		N° Rep.	N		N° Rep.	N
	Di	4	471	Tri	4	49	Tetra	4	7	Penta	4	8
	Di	5	68	Tri	5	12	Tetra	5	1	Penta	5	0
	Di	6	17	Tri	6	5	Tetra	6	1	Penta	6	1
	Di	7	7	Tri	7	2	Tetra	7	1	Penta	7	0
	Di	8	4	Tri	8	0	Tetra	8	0	Penta	8	0
	Di	9	2	Tri	9	0	Tetra	9	0	Penta	9	0
	Di	10	1	Tri	10	2	Tetra	10	0	Penta	10	0
	Di	>10	6	Tri	>10	2	Tetra	>10	0	Penta	>10	0

Table S3: Genetic variability within sites of *Mazzaella laminarioides* for the 12 microsatellite loci. Number of individuals analyzed (*n*); ratio of individuals successfully genotyped (*NI/n*), with *NI* = number of individuals successfully genotyped and *n* = number of individuals analyzed; number of alleles per locus (*Na*); expected heterozygosity (*He*); observed heterozygosity (*Ho*). For each single locus F_{IS} estimates, significant departure from panmixia was tested by running 1,000 permutations of alleles among individuals within sites using GENETIX 4.05 software (Belkhir et al. 1996-2004). F_{IS} values significantly different from zero are shown in bold. Null allele frequency (*Nf*) obtained with MICRO-CHECKER (Oosterhout et al. 2004; Brookfield equation 2, Brookfield 1996), locus showing a significant frequency of null alleles are shown in bold.

	Geographic origin of sampled sites	Northern cytoplasmic lineage		Central cytoplasmic lineage		Southern cytoplasmic lineage		
Loci	Site	SAU	MIT	MTM	LEB	PIL	MLK	All
	n	16	18	16	16	16	14	96
Ml_106C462	*NI/n*	1	1	0.94	1	1	1	0.99
	Na	1	1	1	4	4	4	9
	He	0	0	0	0.23	0.23	0.56	0.76
	Ho	0	0	0	0.13	0.13	0.43	0.11
	F_{IS}	_	_	_	**0.48**	**0.48**	0.27	
	p	_	_	_	**0.03**	**0.04**	0.172	
	Nf	_	_	_	0.08	0.08	0.09	
Ml_106C10	*NI/n*	1	1	1	1	1	1	1
	Na	5	4	3	3	4	3	12
	He	0.33	0.7	0.23	0.53	0.48	0.46	0.81

	Ho	0.31	0.72	0.25	1	0.5	0.64	0.57
	F_{IS}	0.08	0	-0.08	**-0.88**	-0.02	-0.38	
	p	0.389	0.588	0.802	**0**	0.616	0.142	
	Nf	0.01	0	0	0	0	0	
Ml_39C69	*NI/n*	1	1	1	1	0.94	1	0.99
	Na	2	2	3	3	4	5	11
	He	0.22	0.5	0.28	0.54	0.55	0.69	0.83
	Ho	0.25	0.51	0.25	0.38	0.87	0.71	0.57
	F_{IS}	-0.11	**-0.89**	0.12	0.33	**-0.54**	0.01	
	p	0.814	**0.001**	0.316	0.109	**0.014**	0.579	
	Nf	0	0	0.02	0.11	0.08	0	
Ml_106C75	*NI/n*	1	1	1	1	1	1	1
	Na	4	5	4	5	6	4	10
	He	0.54	0.73	0.59	0.54	0.71	0.64	0.81
	Ho	0.25	0.56	0.31	0.31	0.5	0.43	0.4
	F_{IS}	**0.56**	0.26	**0.5**	**0.45**	**0.33**	**0.37**	
	p	**0.006**	0.056	**0.007**	**0.015**	**0.018**	**0.036**	
	Nf	**0.19**	0.1	**0.18**	**0.15**	**0.12**	0.13	
Ml_106C32	*NI/n*	1	1	0.88	1	1	1	0.98
	Na	5	10	9	4	2	4	26
	He	0.56	0.8	0.8	0.5	0.22	0.56	0.87
	Ho	0.63	0.5	0.71	0.19	0.25	0.57	0.47
	F_{IS}	-0.08	**0.4**	0.15	**0.65**	-0.11	0.01	
	p	0.472	**0**	0.183	**0**	0.831	0.576	
	Nf	0	**0.17**	0.26	**0.21**	0	0	
Ml_106C1748	*NI/n*	0.5	0.72	0.38	0.94	0.5	0.93	0.65
	Na	5	7	6	2	8	8	16
	He	0.61	0.83	0.79	0.28	0.83	0.8	0.88

	Ho	0.38	0.69	0.5	0.33	0.75	0.77	0.57
	F_{IS}	0.44	0.21	**0.44**	-0.17	0.16	0.07	
	p	0.055	0.083	**0.03**	0.653	0.226	0.437	
	Nf	0.72	0.45	0.82	0.19	0.66	0.16	
Ml_39C1451	*NI/n*	0.94	1	1	1	1	1	0.99
	Na	3	2	4	2	2	3	4
	He	0.18	0.28	0.56	0.31	0.43	0.52	0.66
	Ho	0.07	0.22	0.57	0.38	0.63	0.64	0.32
	F_{IS}	**0.66**	0.23	**1**	-0.2	-0.43	-0.21	
	p	**0.033**	0.396	**0**	0.582	0.152	0.28	
	Nf	0.28	0.04	**0.36**	0	0	0	
Ml_39C5118	*NI/n*	1	1	1	1	1	1	1
	Na	1	3	4	8	3	2	10
	He	0	0.45	0.59	0.64	0.23	0.5	0.72
	Ho	0	0.47	0.06	0.63	0.25	0.5	0.3
	F_{IS}	_	0.17	**0.9**	0.05	-0.08	0.03	
	p	_	0.304	**0**	0.488	0.8	0.625	
	Nf	_	0.04	**0.33**	0.01	0	0	
Ml_106C203	*NI/n*	1	1	1	1	1	1	1
	Na	1	1	2	2	1	1	2
	He	0	0	0.06	0.26	0	0	0.47
	Ho	0	0	0.06	0.31	0	0	0.06
	F_{IS}	_	_	0	-0.15	_	_	
	p	_	_	0.8	0.682	_	_	
	Nf	_	_	0	0	_	_	
Ml_39C4313	*NI/n*	1	1	0.94	1	1	1	0.99
	Na	5	4	3	2	1	2	6
	He	0.6	0.6	0.29	0.45	0	0.5	0.59

	Ho	0.69	0.28	0.33	0.69	0	1	0.48
	F_{IS}	-0.11	**0.56**	-0.13	-0.5	_	**-1**	
	p	0.396	**0**	0.685	0.075	_	**0**	
	Nf	0	**0.2**	0.19	0	_	0	
Ml_39C37	*NI/n*	1	1	0.88	1	1	0.93	0.97
	Na	4	9	10	4	3	4	23
	He	0.56	0.8	0.84	0.53	0.27	0.7	0.86
	Ho	0.44	0.44	0.64	0.25	0.31	0.31	0.4
	F_{IS}	0.25	**0.47**	**0.27**	**0.55**	-0.12	**0.58**	
	p	0.186	**0**	**0.012**	**0.05**	0.675	**0**	
	Nf	0.08	**0.2**	**0.3**	**0.18**	0	**0.34**	
Ml_106C3942	*NI/n*	1	1	1	1	0.94	1	0.99
	Na	2	2	1	4	2	2	5
	He	0.22	0.11	0	0.61	0.28	0.5	0.63
	Ho	0.13	0.11	0	0.94	0.33	1	0.4
	F_{IS}	**0.46**	-0.03	_	**-0.52**	-0.17	**-1**	
	p	**0.009**	0.978	_	**0.009**	0.679	**0**	
	Nf	0.08	0	_	0	0.19	0	

Table S4: Pairwise multilocus estimates of F_{ST} (θ) (Weir and Cockerham 1984). Values above the diagonal correspond to estimates calculated using the uncorrected 9 loci dataset while the values below the diagonal correspond to estimates calculated using the 9 loci dataset corrected for null alleles using Brookfield equation 2 (Brookfield 1996) implemented in MICRO-CHECKER (Oosterhout et al. 2004). Regardless of the dataset tested, all estimates were associated with significant values of *p*, as assessed by running 1000 permutations using GENETIX 4.05 (Belkhir et al. 1996-2004).

	SAU	MIT	MTM	LEB	PIL	MLK
SAU	–	0.398	0.563	0.549	0.581	0.482
MIT	0.389	–	0.505	0.469	0.537	0.431
MTM	0.562	0.494	–	0.434	0.574	0.402
LEB	0.542	0.457	0.420	–	0.358	0.318
PIL	0.571	0.535	0.571	0.350	–	0.253
MLK	0.479	0.431	0.389	0.312	0.249	–

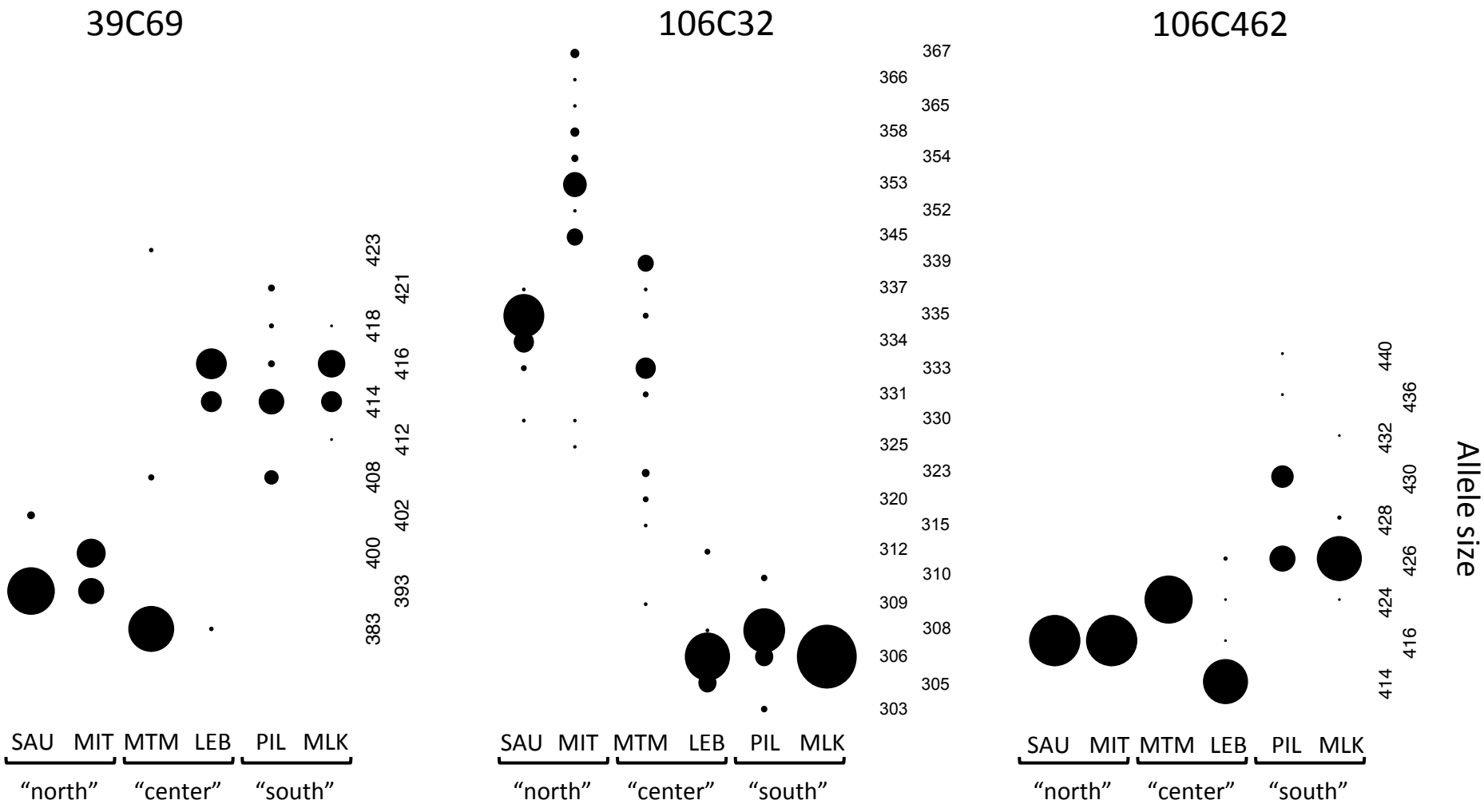

Figure S1: Allele frequency distributions for the nine microsatellite loci observed in each of the six study sites. Sites on the x–axis are ranged from north to south. Numbers on the y-axis are allele sizes in base pairs for each locus. Each circle indicates presence of corresponding allele; diameter of circle represents frequency of that allele in the site. Cytoplasmic lineages (*M. laminarioides* "north", "center" and "south") are noted below the site codes.

Figure S1: Continued from previous page

Figure S2: The posterior probability of the data given K (noted P(X|K), dark circle) and ΔK (white circle) results are given for K = 1 to 7 using the results of the Bayesian analysis obtained with STRUCTURE.

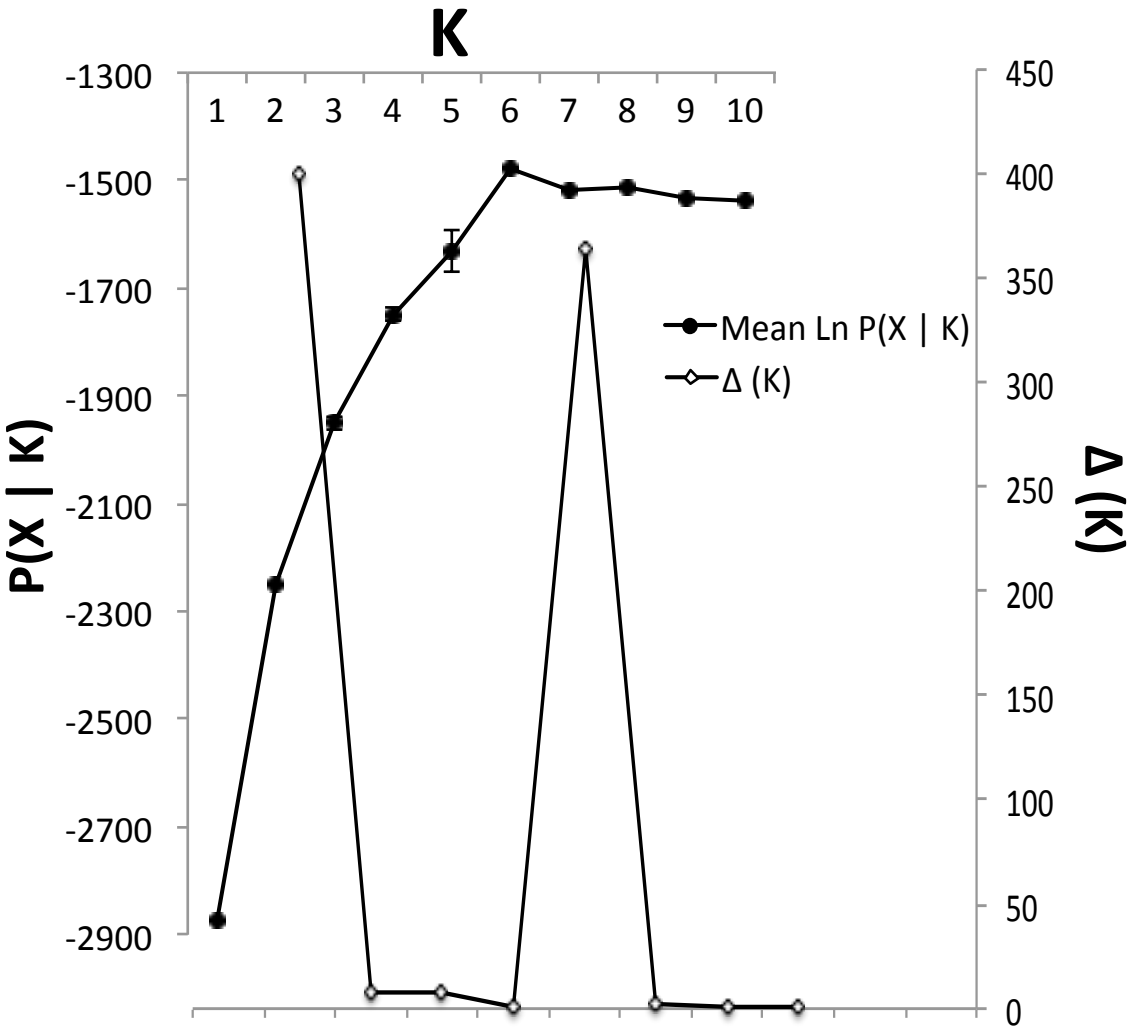

Figure S3: Bayesian analysis using INSTRUCT for the six study sites of *Mazzaella laminarioides*. A) Estimated Deviance Information Criterion (DIC) for values of K = 1 to 7. B) Results of the genetic clustering of the 96 *Mazzaella laminarioides* samples assuming K6. Each vertical bar represents a different individual. Each color represents the proportion of individual genome assigned to each genetic group and * indicates individuals for which a secondary cluster represents more than 5% of the genome (i.e. admixed individuals). Individuals are ordered from north to south.